

A Novel Modifiable Walking Pattern Generator on an Inclined Plane in Pitch and Roll Directions for Humanoid Robots

Young-Dae Hong and Jong-Hwan Kim

Abstract—In previous researches on walking on an inclined plane of humanoid robots including the 3D linear inverted pendulum model (3D-LIPM) approach, the humanoid robots were not able to independently modify walking period and sagittal and lateral step lengths without any additional step for adjusting the center of mass (CM) motion. Moreover, the walking on the inclined plane in pitch direction was only considered. In order to overcome these problems, a novel modifiable walking pattern generator for humanoid robots is proposed for modifiable walking on an inclined plane in both pitch and roll directions. The dynamic equation of the 3D-LIPM on the inclined plane in both pitch and roll directions is derived to obtain the CM motion. Using the CM motion, a method for modifiable walking pattern generation on the inclined plane is developed to follow a navigational command set composed of walking period and sagittal and lateral step lengths. The proposed algorithm is verified through computer simulations carried out with a simulation model of the small-sized humanoid robot, HanSaRam-IX (HSR-IX).

I. INTRODUCTION

For stable walking of humanoid robots, a lot of control algorithms have been developed [1]–[4]. They are on the assumption that the plane is flat. In human environment, however, there exist not only flat but also inclined planes. Therefore, walking on the inclined plane of humanoid robots is one of key research issues in this field.

As research on walking on the inclined plane, there was an approach to measure the inclination of the plane using a foot system, and then walk on the inclined plane by a simple modification of walking motion on a flat plane [5]. Statically stable walking on the inclined plane was studied by maintaining the center of gravity of the humanoid robot within the convex hull of supporting foot [6]. An approach to compute hip height for dynamically stable walking on the inclined plane based on geometric consideration was also introduced [7]. Moreover, preview controller was employed to model the humanoid robot on the inclined plane as a 3D linear inverted pendulum model (3D-LIPM) and generate the trajectory of center of mass (CM) of the 3D-LIPM for walking on the inclined plane [9], [10]. Furthermore, there were some soft computing-based approaches to generate walking motion on the inclined plane by utilizing evolutionary algorithms [11]–[14], neural networks [15]–[21], fuzzy-logic and their combinations [22].

In these previous researches on walking on the inclined plane including the 3D-LIPM approach, the humanoid robots were not able to modify a walking pattern during the single

The authors are with the Department of Electrical Engineering, KAIST, 335 Gwahak-ro, Yuseong-gu, Daejeon 305-701, Republic of Korea (e-mail: {ydhong, johkim}@rit.kaist.ac.kr).

support phase. Namely, it was impossible to independently change the walking pattern, i.e. walking period and sagittal and lateral step lengths on the inclined plane without any additional step for adjusting the CM motion. Moreover, the walking on the inclined plane in pitch direction was only considered. In real environments, however, there exist inclined planes in roll as well as pitch directions.

In order to overcome these problems, this paper proposes a novel modifiable walking pattern generator (MWPG) for humanoid robots. The proposed MWPG is based on conventional MWPG which has two closed form functions to allow zero moment point (ZMP) variation in real-time [23]. However, the conventional MWPG can be only applied on the flat plane to modify walking period and sagittal and lateral step lengths independently. Thus, in this paper, the novel MWPG is proposed to be applied on the inclined plane in both pitch and roll directions. Initially, the dynamic equation of the 3D-LIPM on the inclined plane in both pitch and roll directions is derived to obtain the CM motion with ZMP functions. Using the CM motion, a method for modifiable walking pattern generation on the inclined plane is developed to follow a navigational command set composed of walking period and sagittal and lateral step lengths, which called command state (CS). Once the CS is entered, it is converted into desired walking state (WS) defined by the position and velocity of the CM in sagittal and lateral planes. Next, the control parameters for ZMP functions are obtained to guarantee the desired WS is achievable. The proposed algorithm is verified through computer simulations carried out with a simulation model of the small-sized humanoid robot, HanSaRam-IX (HSR-IX), developed at the Robot Intelligence Technology (RIT) laboratory, KAIST.

This paper is organized as follows: Section II presents the dynamics of the 3D-LIPM on the inclined plane in both pitch and roll directions, and the CM motion equations of the 3D-LIPM on the inclined plane are derived. In Section III, a method for modifiable walking pattern generation on the inclined plane is developed to follow a entered CS. Section IV presents computer simulation results and finally conclusions follow in Section V.

II. 3D-LIPM ON INCLINED PLANE IN PITCH AND ROLL DIRECTIONS

A. Dynamics of 3D-LIPM

The primary dynamics of walking of a humanoid robot on a flat plane can be modeled as a single inverted pendulum which is called the 3D linear inverted pendulum model (3D-LIPM) [24]. It is assumed that the leg is a weightless

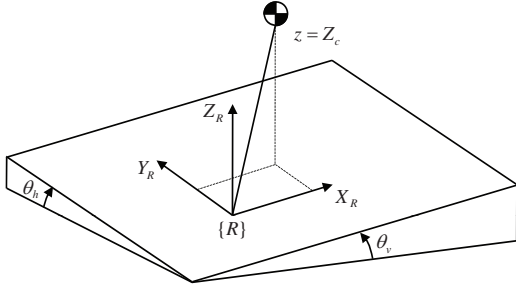


Fig. 1. 3D-LIPM on inclined plane in pitch and roll directions.

telescopic limb and the mass is concentrated as a single point without vertical motion. Thus, the motion equations for the sagittal and lateral planes can be decoupled. The 3D-LIPM can be extended to on the inclined plane in pitch and roll directions as shown in Fig. 1. The dynamic equation of the 3D-LIPM for the angular momentum taken around the contact point between the pendulum model and ground surface in the frame $\{R\}$ is written as follows:

$$\mathbf{T}_{gr} + \mathbf{r}_{cm} \times \mathbf{F}_{gr} = \frac{d}{dt}(\mathbf{r}_{cm} \times \mathbf{L}) \quad (1)$$

where $\mathbf{T}_{gr} = [T_x \ T_y \ T_z]^T$ represents the torque created by the ground reaction force, $\mathbf{r}_{cm} = [x \ y \ z]^T$ represents the vector from the contact point to the CM, and \mathbf{L} is the linear momentum of the CM. Gravitational force \mathbf{F}_{gr} are given as

$$\mathbf{F}_{gr} = \begin{bmatrix} -mg \sin \theta_v \\ -mg \sin \theta_h \\ -mg \cos \theta_v \cos \theta_h \end{bmatrix} \quad (2)$$

where m is the mass of the pendulum. θ_v and θ_h represent the pitch and roll angles of the inclined plane, respectively. If θ_v is positive/negative, the plane is inclined upward/downward. Similarly, if θ_h is positive/negative, the plane is inclined leftside/rightside. Since the height of the CM, z is constant Z_c , (1) can be rewritten as follows:

$$\begin{bmatrix} \ddot{y} - \frac{g \cos \theta_v \cos \theta_h}{Z_c} y + g \sin \theta_h \\ \ddot{x} - \frac{g \cos \theta_v \cos \theta_h}{Z_c} x + g \sin \theta_v \end{bmatrix} = \begin{bmatrix} -\frac{T_x}{mZ_c} \\ \frac{T_y}{mZ_c} \end{bmatrix} \quad (3)$$

The ZMP is used to represent the sum of the torques caused by the ground reaction force as follows:

$$\mathbf{T}_{gr} - \mathbf{r}_{zmp} \times \mathbf{F}_{gr} = [0 \ 0 \ M_z]^T \quad (4)$$

where $\mathbf{r}_{zmp} = [x_{zmp} \ y_{zmp} \ 0]^T$ represents the ZMP and M_z denotes the yaw moment. T_x and T_y are obtained from (4), and then the following dynamic equation of the 3D-LIPM can be obtained by substituting them into (3):

$$\begin{bmatrix} \ddot{y} - \frac{g \cos \theta_v \cos \theta_h}{Z_c} y + g \sin \theta_h \\ \ddot{x} - \frac{g \cos \theta_v \cos \theta_h}{Z_c} x + g \sin \theta_v \end{bmatrix} = -\frac{g \cos \theta_v \cos \theta_h}{Z_c} \begin{bmatrix} y_{zmp} \\ x_{zmp} \end{bmatrix}. \quad (5)$$

The above equation provides the relationship between the ZMP and the CM motion of the 3D-LIPM on the inclined plane in pitch and roll directions.

B. CM Motion Equations of 3D-LIPM

By applying inverse Laplace transform, the solutions of (5), which mean the CM motion of the 3D-LIPM on the inclined plane, are obtained as follows:

Sagittal motion:

$$\begin{bmatrix} x_f \\ v_f T_c \end{bmatrix} = \begin{bmatrix} \cosh(\frac{T}{T_c}) & \sinh(\frac{T}{T_c}) \\ \sinh(\frac{T}{T_c}) & \cosh(\frac{T}{T_c}) \end{bmatrix} \begin{bmatrix} x_i \\ v_i T_c \end{bmatrix} - \frac{1}{T_c} \begin{bmatrix} \int_0^T \sinh(\frac{T}{T_c}) \bar{p}(t) dt \\ \int_0^T \cosh(\frac{T}{T_c}) \bar{p}(t) dt \end{bmatrix} + \begin{bmatrix} -gT_c^2 \sin \theta_v (-1 + \cosh(\frac{T}{T_c})) \\ -gT_c^2 \sin \theta_v \sinh(\frac{T}{T_c}) \end{bmatrix} \quad (6)$$

Lateral motion:

$$\begin{bmatrix} y_f \\ w_f T_c \end{bmatrix} = \begin{bmatrix} \cosh(\frac{T}{T_c}) & \sinh(\frac{T}{T_c}) \\ \sinh(\frac{T}{T_c}) & \cosh(\frac{T}{T_c}) \end{bmatrix} \begin{bmatrix} y_i \\ w_i T_c \end{bmatrix} - \frac{1}{T_c} \begin{bmatrix} \int_0^T \sinh(\frac{T}{T_c}) \bar{q}(t) dt \\ \int_0^T \cosh(\frac{T}{T_c}) \bar{q}(t) dt \end{bmatrix} + \begin{bmatrix} -gT_c^2 \sin \theta_h (-1 + \cosh(\frac{T}{T_c})) \\ -gT_c^2 \sin \theta_h \sinh(\frac{T}{T_c}) \end{bmatrix} \quad (7)$$

with

$$T_c = \sqrt{\frac{Z_c}{g \cos \theta_v \cos \theta_h}}$$

where $(x_i, v_i)/(x_f, v_f)$ and $(y_i, w_i)/(y_f, w_f)$ represent the initial/final position and velocity of the CM in sagittal and lateral planes, respectively. T is the remaining single support time. $p(t)$ and $q(t)$ are the ZMP functions for sagittal and lateral motions, respectively. $\bar{p}(t) = p(T - t)$ and $\bar{q}(t) = q(T - t)$. In terms of implementation, $p(t)$ and $q(t)$ are selected as the constant function and the step function, respectively, among infinitely many candidate functions as follows [23]:

$$p(t) = \begin{cases} P, & \text{if } 0 \leq t < T \\ 0, & \text{otherwise} \end{cases}, \quad q(t) = \begin{cases} Q, & \text{if } 0 \leq t < T_{sw} \\ -Q, & \text{if } T_{sw} \leq t \leq T \end{cases} \quad (8)$$

where P and Q are the magnitudes of constant and step functions, respectively. T_{sw} is the switching time of step function.

The first terms on the right-hand side of (6) and (7) indicate homogeneous solutions of (5). The second terms represent additional states (particular solutions) that allow more extensive and unrestricted motions by varying ZMP trajectories with $p(t)$ and $q(t)$. In the conventional 3D-LIPM approach, the particular solutions have not been considered, assuming that the ZMP is fixed at the contact point. Consequently, the dynamics for the CM motion of the 3D-LIPM is predetermined and unmodifiable throughout the single support phase. Thus, it is impossible to modify a walking pattern, i.e. walking period and sagittal and lateral step lengths independently in the conventional 3D-LIPM. The last terms perform shifting the CM trajectory of the 3D-LIPM for

walking on the inclined plane according to the pitch and roll angles of the inclined plane (θ_v and θ_h).

To formulate the state of the CM of the 3D-LIPM, walking state (WS) is defined with the position and velocity of the CM in sagittal and lateral planes as follows [23]:

Definition 1: Walking state (WS) is defined as

$$\mathbf{x} = [x \quad T_c v]^T \text{ for sagittal motion;}$$

$$\mathbf{y} = [y \quad T_c w]^T \text{ for lateral motion.}$$

Note that the WS is represented as a two dimensional vector in each plane and the velocity terms are multiplied with T_c .

III. METHOD FOR MODIFIABLE WALKING PATTERN GENERATION ON INCLINED PLANE IN PITCH AND ROLL DIRECTIONS

A. Command State

In order to generate a walking pattern, a minimal navigational command set is required. For this purpose, command state (CS) is defined, which includes single and double support times and sagittal and lateral step lengths as follows [23]:

Definition 2: Command state (CS) is defined as

$$\mathbf{c} \equiv [T_{ss} \quad T_{ds} \quad W_S \quad W_{Ll} \quad W_{Lr}]$$

where

- T_{ss} : single support time;
- T_{ds} : double support time;
- W_S : sagittal step length;
- W_{Ll} : lateral step length of left leg;
- W_{Lr} : lateral step length of right leg.

B. Conversion of Command State into Desired Walking State

Walking of the robot can be described by identifying the WSs at particular points in motion because it is a repetitive motion. When the robot follows a entered CS, it is assumed that the robot's state is in steady state and ZMP variation is not utilized. These assumptions correspond directly to a walking pattern that represents a steady state motion for the 3D-LIPM, in which the particular solutions of (6) and (7) are zero and only homogenous solutions are used. In this situation, the WS at the end of each single support phase is identical. This state is called as desired WS.

To convert the CS into the desired WS, it is enough to observe just one period of walking configuration in steady state as shown in Fig 2. Since the robot's state is in steady state without ZMP variation, walking configuration can be fully described by initial or final WS for both left and right leg support phases. In terms of implementation, the CM is controlled to travel with constant velocity during double support phase for a specific time T_{ds} .

Notation 1: In the derivation, the following notations are used:

- \mathbf{x}_{li} : initial WS of sagittal motion for left support phase;
- \mathbf{x}_{lf} : final WS of sagittal motion for left support phase;
- \mathbf{x}_{ri} : initial WS of sagittal motion for right support phase;
- \mathbf{x}_{rf} : final WS of sagittal motion for right support phase;

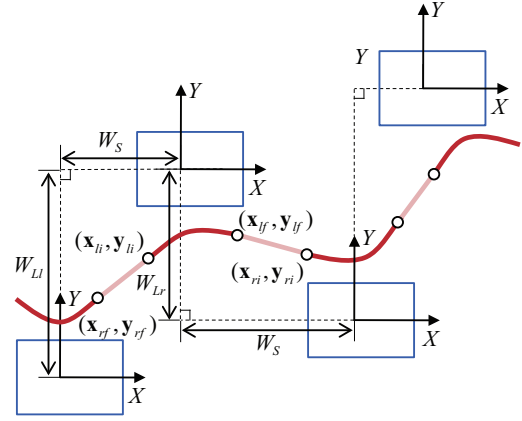


Fig. 2. Walking configuration in steady state.

- \mathbf{y}_{li} : initial WS of lateral motion for left support phase;
- \mathbf{y}_{lf} : final WS of lateral motion for left support phase;
- \mathbf{y}_{ri} : initial WS of lateral motion for right support phase;
- \mathbf{y}_{rf} : final WS of lateral motion for right support phase.

Note that each WS is defined with respect to the local coordinate frame attached on its support leg.

1) *Sagittal Motion:* From the equation for the sagittal motion, (6) with $\bar{p}(t) = 0$ and $\bar{q}(t) = 0$, the following two state equations are obtained during single support phase, which represent left and right single support phases, respectively:

$$\mathbf{x}_{lf} = \mathbf{A}\mathbf{x}_{li} + \mathbf{B}, \quad \mathbf{x}_{rf} = \mathbf{A}\mathbf{x}_{ri} + \mathbf{B} \quad (9)$$

where

$$\mathbf{A} = \begin{bmatrix} \cosh\left(\frac{T_{ss}}{T_c}\right) & \sinh\left(\frac{T_{ss}}{T_c}\right) \\ \sinh\left(\frac{T_{ss}}{T_c}\right) & \cosh\left(\frac{T_{ss}}{T_c}\right) \end{bmatrix}$$

$$\mathbf{B} = \begin{bmatrix} -gT_c^2 \sin \theta_v (-1 + \cosh\left(\frac{T_{ss}}{T_c}\right)) \\ -gT_c^2 \sin \theta_v \sinh\left(\frac{T_{ss}}{T_c}\right) \end{bmatrix}.$$

During double support phase, the following two equations are given because the velocity of the CM is controlled to be constant in double support phase as mentioned above:

$$\mathbf{x}_{li} = \mathbf{C}\mathbf{x}_{rf} + \mathbf{D}, \quad \mathbf{x}_{ri} = \mathbf{C}\mathbf{x}_{lf} + \mathbf{D} \quad (10)$$

where

$$\mathbf{C} = \begin{bmatrix} 1 & T_{ds}/T_c \\ 0 & 1 \end{bmatrix}, \quad \mathbf{D} = \begin{bmatrix} -W_S \\ 0 \end{bmatrix}.$$

From (9) and (10), sagittal steady state motion of the CM can be expressed by

$$\mathbf{x}_{lf} = \mathbf{x}_{rf} = (\mathbf{I} - \mathbf{AC})^{-1}(\mathbf{AD} + \mathbf{B}) \quad (11)$$

where \mathbf{I} is the identity matrix. This equation explains the mapping relationship between the CS and the desired WS. That is, once the CS is arrived, it is converted into the desired WS form. The information of the CS is involved in the matrices \mathbf{A} , \mathbf{B} , \mathbf{C} , and \mathbf{D} .

2) *Lateral Motion*: By the same process, the following four equations are obtained for lateral motion:

$$\begin{aligned} \mathbf{y}_{lf} &= \mathbf{A}\mathbf{y}_{li} + \mathbf{B}, & \mathbf{y}_{rf} &= \mathbf{A}\mathbf{y}_{ri} + \mathbf{B} \\ \mathbf{y}_{li} &= \mathbf{C}\mathbf{y}_{rf} + \mathbf{D}, & \mathbf{y}_{ri} &= \mathbf{C}\mathbf{y}_{lf} + \mathbf{E} \end{aligned} \quad (12)$$

where

$$\begin{aligned} \mathbf{A} &= \begin{bmatrix} \cosh(\frac{T_{ss}}{T_c}) & \sinh(\frac{T_{ss}}{T_c}) \\ \sinh(\frac{T_{ss}}{T_c}) & \cosh(\frac{T_{ss}}{T_c}) \end{bmatrix} \\ \mathbf{B} &= \begin{bmatrix} -gT_c^2 \sin \theta_h (-1 + \cosh(\frac{T_{ss}}{T_c})) \\ -gT_c^2 \sin \theta_h \sinh(\frac{T_{ss}}{T_c}) \end{bmatrix} \end{aligned}$$

$$\mathbf{C} = \begin{bmatrix} 1 & T_{ds}/T_c \\ 0 & 1 \end{bmatrix}, \quad \mathbf{D} = \begin{bmatrix} -W_{Ll} \\ 0 \end{bmatrix}, \quad \mathbf{E} = \begin{bmatrix} W_{Lr} \\ 0 \end{bmatrix}.$$

Subsequently, lateral steady state motion of the CM can be expressed by

$$\begin{aligned} \mathbf{y}_{lf} &= (\mathbf{I} - (\mathbf{AC})^2)^{-1}(\mathbf{ACAE} + \mathbf{AD} + \mathbf{ABC} + \mathbf{B}) \\ \mathbf{y}_{rf} &= (\mathbf{I} - (\mathbf{AC})^2)^{-1}(\mathbf{ACAD} + \mathbf{AE} + \mathbf{ABC} + \mathbf{B}). \end{aligned} \quad (13)$$

C. Control Parameters

The control parameters T , P , T_{sw} , and Q , which characterize the ZMP functions, should be solved to guarantee that desired WS is achievable. Here, T represents the remaining time in single support for current step to achieve the desired WS.

1) *Control Parameters for Sagittal Motion*: From the equation for the sagittal motion, (6) with $t = T$ and $p(t) = P$, the control parameters T and P are obtained as follows:

$$\begin{aligned} T &= T_c \ln \left(\frac{(v_d + v_i)T_c + (x_d - x_i)}{(v_d + v_i)T_c - (x_d - x_i)} \right) \\ P &= \frac{(x_d^2 - x_i^2) - (v_d^2 - v_i^2)T_c^2}{2(x_d - x_i)} - gT_c^2 \sin \theta_v \end{aligned} \quad (14)$$

where $[x_d \ T_c v_d]^T$ represents desired WS.

2) *Control Parameters for Lateral Motion*: The homogeneous part of the equation for the lateral motion, (7) is determined by initial WS and the pre-calculated T from the equation for the sagittal motion. Therefore, it is only necessary to consider the particular solution. The particular solution of the equation for the lateral motion is derived from (7) as

$$\begin{bmatrix} y_p \\ T_c w_p \end{bmatrix} = \begin{bmatrix} 2 \cosh(\frac{T - T_{sw}}{T_c}) - (1 + \cosh(\frac{T}{T_c})) \\ 2 \sinh(\frac{T - T_{sw}}{T_c}) - \sinh(\frac{T}{T_c}) \end{bmatrix} Q. \quad (15)$$

From (15), T_{sw} and Q are obtained as follows:

$$\begin{aligned} T_{sw} &= T - T_c \ln(h), \quad 0 \leq T_{sw} \leq T \\ Q &= \frac{y_p}{(h + h^{-1}) - (1 + \cosh(\frac{T}{T_c}))} \end{aligned} \quad (16)$$

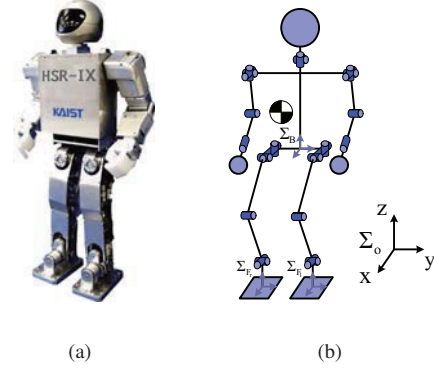


Fig. 3. Humanoid robot. (a) HanSaRam-IX. (b) Configuration.

where

$$\begin{aligned} h &= \begin{cases} \frac{\gamma + \sqrt{\gamma^2 + 4\alpha\beta}}{2\alpha}, & \text{if } \delta < 0 \\ 1, & \text{if } \delta = 0 \\ \frac{\gamma - \sqrt{\gamma^2 + 4\alpha\beta}}{2\alpha}, & \text{if } \delta > 0 \end{cases} \\ \alpha &= y_p - T_c w_p, \quad \beta = y_p + T_c w_p \\ \gamma &= y_p \sinh(\frac{T}{T_c}) - T_c w_p (1 + \cosh(\frac{T}{T_c})) \\ \delta &= y_p \sinh(\frac{T}{T_c}) + T_c w_p (1 - \cosh(\frac{T}{T_c})). \end{aligned}$$

From (14) and (16), the control parameters are directly calculated from the current and the desired WSs.

D. Overall Procedure

It is assumed that the pitch and roll angles of the inclined plane are measurable in this paper. A CS is entered into the proposed algorithm for each sample time. Then, it is converted into desired WS using (11) and (13). Next, control parameters T , P , T_{sw} , and Q for ZMP functions are calculated to get the desired WS from (14) and (16), and then the WS is calculated using (6) and (7). Subsequently, the CM motion is updated. Trajectories of every leg joint are calculated by inverse kinematics.

IV. COMPUTER SIMULATIONS

The proposed algorithm was implemented on the simulation model of the small-sized humanoid robot, HanSaRam-IX (HSR-IX) (Fig. 3(a)). HSR-IX has been in continual development and research by the RIT laboratory, KAIST [4]. Its height and weight are 52.8 cm and 5.5 kg, respectively. It has 26 DOFs which consist of 12 DC motors with harmonic drives in the lower body and 16 RC servo motors in the upper body (Fig. 3(b)). The on-board Pentium-III compatible PC, running RT-Linux, calculates the proposed algorithm every 5 msec in real-time. To measure ground reaction forces on the feet and the real ZMP trajectories while walking, four force sensing resistors (FSR) are equipped on each foot.

The simulation model of HSR-IX was modeled by Webot which is the 3D robotics simulation software and enables users to conduct the physical and dynamical simulation [25].

In order to verify the modifiable walking on the inclined plane in pitch and roll directions, the following CS list for the simulations was used, in which sagittal and lateral step lengths were independently changed while maintaining the same walking period at each footstep:

- Initial CS, $\mathbf{c} = [0.8 \ 0.4 \ 4.0 \ 6.0 \ -6.0]$
- After 2nd step, $\mathbf{c} = [0.8 \ 0.4 \ 1.0 \ 6.0 \ -10.0]$
- After 3rd step, $\mathbf{c} = [0.8 \ 0.4 \ 4.0 \ 6.0 \ -6.0]$
- After 5th step, $\mathbf{c} = [0.8 \ 0.4 \ 2.0 \ 9.0 \ -6.0]$
- After 6th step, $\mathbf{c} = [0.8 \ 0.4 \ 4.0 \ 6.0 \ -6.0]$
- After 9th step, $\mathbf{c} = [0.8 \ 0.4 \ 2.0 \ 9.0 \ -6.0]$
- After 10th step, $\mathbf{c} = [0.8 \ 0.4 \ 4.0 \ 6.0 \ -6.0]$
- After 12th step, $\mathbf{c} = [0.8 \ 0.4 \ 0.0 \ 6.0 \ -6.0]$

where time units and length units were given in seconds and centimeters, respectively.

Fig. 4 shows the generated walking pattern and CM trajectories using the proposed algorithm for walking when the plane was inclined upward ($\theta_v = 15^\circ$), downward ($\theta_v = -15^\circ$), leftside ($\theta_h = 5^\circ$), and rightside ($\theta_h = -5^\circ$). In the simulation, allowable pitch and roll plane angles were from -20.0° to 20.0° and from -8.0° to 8.0° , respectively, for the robot to walk straight while maintaining stability. In the figure, the thick line represents the generated CM trajectory and the thin line represents the foot boundary. The small circle represents the foot position satisfying the commanded CS list. As shown in the figure, the robot followed the entered CS list successfully. When the plane was inclined upward/downward, the CM trajectory which was shifted forward/backward compared to that on the flat plane was generated. Similarly, when the plane was inclined leftside/rightside, the CM trajectory which was shifted left/right was generated. Thus, by means of generating the shifted CM trajectory like them, the robot was able to walk stably on the inclined plane because the ZMP was within the foot boundary.

Fig. 5 shows the generated walking pattern, CM, and ZMP trajectories when the plane was inclined upward and leftside simultaneously ($\theta_v = 15^\circ$ and $\theta_h = 5^\circ$). As the figure shows, the CM trajectory which was shifted forward and left simultaneously was generated for stable walking. The ZMP on xy plane was within the boundary of the support foot during single support phase and moved from the current support foot to the next support foot during double support phase. Moreover, it can be shown that the ZMP trajectories in x -axis and y -axis follow the foot trajectories with a small variation. The small variation was mainly caused by the dynamic difference between the robot and the 3D-LIPM. However, the ZMP trajectories were within the upper and lower boundaries of foot trajectories. Accordingly, the robot was able to walk stably on the inclined plane in both pitch and roll directions (See the accompanying video).

V. CONCLUSION

In this paper, a novel modifiable walking pattern generator for humanoid robots was proposed for modifiable walking on the inclined plane in both pitch and roll directions. The proposed algorithm independently changed walking period

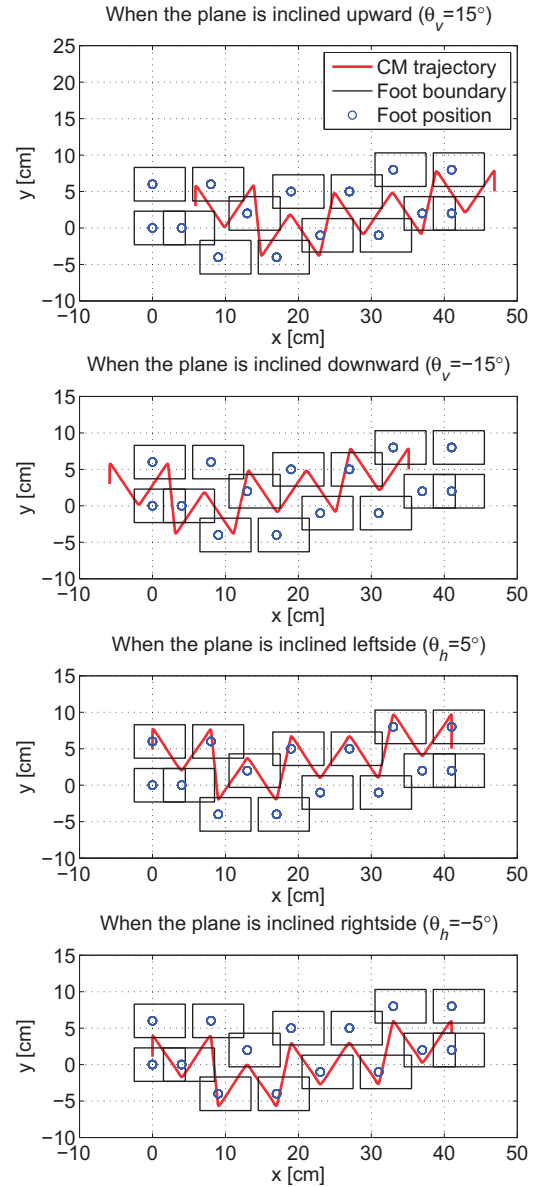


Fig. 4. Generated walking pattern and CM trajectories using the proposed algorithm.

and sagittal and lateral step lengths on the inclined plane without any additional step for adjusting the CM motion. The CM motion equations of the 3D-LIPM with ZMP functions were obtained by deriving the dynamic equation of the 3D-LIPM on the inclined plane. From the CM motion equations, the method for modifiable walking pattern generation on the inclined plane was developed. The CS was defined and once it was entered, it was converted into the desired WS. Moreover, control parameters for ZMP functions were obtained to guarantee the desired WS is achievable. The effectiveness of the proposed algorithm was demonstrated through computer simulations carried out with the simulation model of the small-sized humanoid robot, HSR-IX. Consequently, by using the proposed algorithm, the humanoid robot

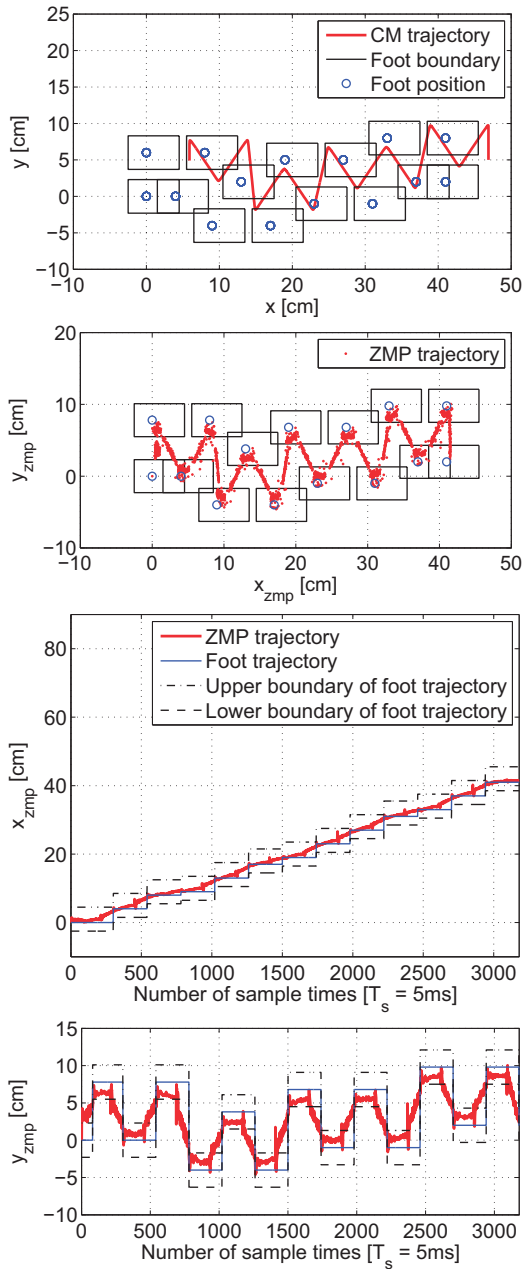


Fig. 5. Generated walking pattern, CM, and ZMP trajectories when the plane was inclined upward and leftside simultaneously in the simulation ($\theta_v = 15^\circ$ and $\theta_h = 5^\circ$).

could walk stably on the inclined plane in both pitch and roll directions following the commanded CS list in which sagittal and lateral step lengths were independently changed while maintaining the same walking period at each footstep.

VI. ACKNOWLEDGMENTS

This research was supported by Basic Science Research Program through the National Research Foundation of Korea (NRF) funded by the Ministry of Education, Science and Technology (2010-0000831).

REFERENCES

- [1] Y. Sakagami, R. Watanabe, C. Aoyama, S. Matsunaga, N. Higaki, and K. Fujimura, "The intelligent ASIMO: system overview and integration," in *Proc. IEEE/RSJ Int. Conf. Intell. Robot. Syst.*, 2002, pp. 2478–2483.
- [2] K. Akachi, K. Kaneko, N. Kanehira, S. Ota, G. Miyamori, M. Hirata, S. Kajita, and F. Kanehiro, "Development of humanoid robot HRP-3P," in *Proc. IEEE-RAS Int. Conf. Humanoid Robots*, 2005, pp. 50–55.
- [3] I.-W. Park, J.-Y. Kim, J. Lee, and J.-H. Oh, "Online free walking trajectory generation for biped humanoid robot KHR-3(HUBO)," in *Proc. IEEE Int. Conf. Robot. Autom.*, 2006, pp. 1231–1236.
- [4] J.-K. Yoo, B.-J. Lee, and J.-H. Kim, "Recent progress and development of the humanoid robot HanSaRam," *Robot. Auton. Syst.*, vol. 57, no. 10, pp. 973–981, 2009.
- [5] Y. F. Zheng and J. Shen, "Gait synthesis for the SD-2 biped robot to climb sloping surface," *IEEE Trans. Robot. Autom.*, vol. 6, no. 1, pp. 86–96, 1990.
- [6] C.-L. Shih and C.-J. Chiou, "The motion control of a statically stable biped robot on an uneven floor," *IEEE Trans. Syst. Man, Cybern. B, Cybern.*, vol. 28, no. 2, pp. 244–249, 1998.
- [7] C.-M. Chew, J. Pratt, and G. Pratt, "Blind walking of a planar bipedal robot on sloped terrain," in *Proc. IEEE Int. Conf. Robot. Autom.*, 1999, vol. 1, pp. 381–386.
- [8] M. Ogino, H. Toyama, and M. Asada, "Stabilizing biped walking on rough terrain based on the compliance control," in *Proc. IEEE/RSJ Int. Conf. Intell. Robot. Syst.*, 2007, pp. 4047–4052.
- [9] S. Kajita, F. Kanehiro, K. Kaneko, K. Fujiwara, K. Harada, K. Yokoi, and H. Hirukawa, "Biped walking pattern generation by using preview control of zero-moment point," in *Proc. IEEE Int. Conf. Robot. Autom.*, 2003, vol. 2, pp. 1620–1626.
- [10] W. Huang, C.-M. Chew, Y. Zheng, and G.-S. Hong, "Pattern generation for bipedal walking on slopes and stairs," in *Proc. IEEE-RAS Int. Conf. Humanoid Robots*, 2008, pp. 205–210.
- [11] M.-Y. Cheng and C.-S. Lin, "Genetic algorithm for control design of biped locomotion," *J. Robot. Syst.*, vol. 14, no. 5, pp. 365–373, 1997.
- [12] M.-Y. Cheng and C.-S. Lin, "Dynamic biped robot locomotion on less structured surfaces," *Robotica*, vol. 18, pp. 163–170, 2000.
- [13] Y. Hasegawa, T. Arakawa, and T. Fukuda, "Trajectory generation for biped locomotion robot," *Mechatronics*, vol. 10, pp. 67–89, 2000.
- [14] L. Yang, C.-M. Chew, T. Zielinska, and A.-N. Poo, "A uniform biped gait generator with offline optimization and online adjustable parameters," *Robotica*, vol. 25, pp. 549–565, 2007.
- [15] G. Taga, Y. Yamaguchi, and H. Shimizu, "Self-organized control of bipedal locomotion by neural oscillators in unpredictable environment," *Biol. Cybern.*, vol. 65, no. 3, pp. 147–159, 1991.
- [16] A. W. Salatian and Y. F. Zheng, "Gait synthesis for a biped robot climbing sloping surfaces using neural networks. I. Static learning," in *Proc. IEEE Int. Conf. Robot. Autom.*, 1992, vol. 3, pp. 2601–2606.
- [17] A. W. Salatian and Y. F. Zheng, "Gait synthesis for a biped robot climbing sloping surfaces using neural networks. II. Dynamic learning," in *Proc. IEEE Int. Conf. Robot. Autom.*, 1992, vol. 3, pp. 2607–2611.
- [18] A. W. Salatian, K. Y. Yi, and Y. F. Zheng, "Reinforcement learning for a biped robot to climb sloping surfaces," *J. Robot. Syst.*, vol. 14, no. 4, pp. 283–296, 1997.
- [19] J.-G. Juang, "Intelligent locomotion control on sloping surfaces," *Information Sciences*, vol. 147, pp. 229–243, 2002.
- [20] K. Tsuchiya, S. Aoi, and K. Tsujita, "Locomotion control of a biped locomotion robot using nonlinear oscillators," in *Proc. IEEE/RSJ Int. Conf. Intell. Robot. Syst.*, 2003, vol. 2, pp. 1745–1750.
- [21] S. Aoi and K. Tsuchiya, "Locomotion control of a biped robot using nonlinear oscillators," *Auton. Robots*, vol. 19, no. 3, pp. 219–232, 2005.
- [22] P. R. Vundavilli and D. K. Pratihari, "Soft computing-based gait planners for a dynamically balanced biped robot negotiating sloping surfaces," *Applied Soft Computing Journal*, vol. 9, no. 1, pp. 191–208, 2009.
- [23] B.-J. Lee, D. Stonier, Y.-D. Kim, J.-K. Yoo, and J.-H. Kim, "Modifiable walking pattern of a humanoid robot by using allowable ZMP variation," *IEEE Trans. Robot.*, vol. 24, no. 4, pp. 917–925, 2008.
- [24] S. Kajita, F. Kanehiro, K. Kaneko, K. Fujiwara, K. Yokoi, and H. Hirukawa, "A realtime pattern generator for biped walking," in *Proc. IEEE Int. Conf. Robot. Autom.*, 2002, vol. 1, pp. 31–37.
- [25] O. Michel, "Cyberbotics Ltd. WebotsTM: Professional mobile robot simulation," *Int. J. Advanced Robot. Syst.*, vol. 1, no. 1, pp. 39–42, 2004.